

Wehrl Entropy and Entanglement Complexity of Quantum Spin Systems

Chen Xu,¹ Yiqi Yu,¹ and Peng Zhang^{1,2,3,*}

¹Department of Physics, Renmin University of China, Beijing, 100872, China

²Key Laboratory of Quantum State Construction and Manipulation (Ministry of Education),
Renmin University of China, Beijing, 100872, China

³Beijing Key Laboratory of Opto-electronic Functional Materials & Micro-nano Devices (Renmin University of China)

(Dated: today)

The Wehrl entropy of a quantum state is the entropy of the coherent-state distribution function (Husimi function) of this state. This entropy is non-zero even for pure states. We investigate the Wehrl entropy for N spin-1/2 particles with respect to the $SU(2)^{\otimes N}$ coherent states (*i.e.*, the direct products of spin coherent states of each particle). We focus on: (1) The statistical interpretation of this Wehrl entropy. (2) The relationship between the Wehrl entropy and quantum entanglement, particularly in systems with a large number of particles. For the problem (1), despite the coherent states not forming a group of orthonormal bases, we prove that the Wehrl entropy can still be interpreted as the entropy of a probability distribution with clear physical meaning. For the problem (2), we numerically calculate the Wehrl entropy of various types of entangled pure states with respect to particle number $2 \leq N \leq 20$. Our results show that for the large- N ($N \gtrsim 10$) systems the Wehrl entropy of the highly chaotic entangled states (*e.g.*, $2^{-N/2} \sum_{s_1, s_2, \dots, s_N = \uparrow, \downarrow} |s_1, s_2, \dots, s_N\rangle e^{-i\phi_{s_1, s_2, \dots, s_N}}$, with $\phi_{s_1, s_2, \dots, s_N}$ being 2^N random angles) are substantially larger than that of the very regular ones (*e.g.*, the Greenberger–Horne–Zeilinger state). These results, together with the fact that the Wehrl entropy is invariant under local unitary transformations, indicate that the Wehrl entropy can reflect the complexity of the quantum entanglement (entanglement complexity) of many-body pure states, as A. Sugita proposed directly from the definitions of the Husimi function and Wehrl entropy (Jour. Phys. A **36**, 9081 (2003)). Furthermore, the Wehrl entropy per particle can serve as a quantitative description of this entanglement complexity. We further show that the many-body pure entangled states can be classified into three types, according to the behaviors of the Wehrl entropy per particle in the limit $N \rightarrow \infty$, with the states of each type having very different entanglement complexity. Therefore, the Wehrl entropy is helpful for the research areas related to the entanglement complexity of a many-body system, such as many-body quantum dynamics, spin-liquids and quantum computation.

I. INTRODUCTION

Entropy plays a crucial role in various fields of physics, including but not limited to statistical mechanics, quantum information, many-body physics, and quantum chaos [1–6]. The Wehrl entropy was initially proposed by A. Wehrl in 1979 [7]. For a given quantum system with density operator $\hat{\rho}$, the Wehrl entropy is defined as the entropy of the Husimi function $\langle \mathbf{n} | \hat{\rho} | \mathbf{n} \rangle / Z$ [8], where $\{|\mathbf{n}\rangle\}$ are the coherent states of this system and $Z = \int d\mathbf{n} \langle \mathbf{n} | \hat{\rho} | \mathbf{n} \rangle$ serves as the normalization constant. For instance, for a single spin-1/2 particle, $\{|\mathbf{n}\rangle\}$ are the $SU(2)$ spin-coherent states, where \mathbf{n} is a three-dimensional (3D) unit vector, *i.e.*, $\mathbf{n} \in S^2$ with S^2 being the unit sphere (Bloch sphere) of the 3D space. Unlike the well-known von Neumann entropy, the Wehrl entropy is non-zero even for a pure state, and can change with time during the evolution of a closed system. The Wehrl entropy has been applied and studied in various fields such as quantum optics [9, 10], quantum information [11] and mathematical physics [12–15].

For the system of N spin-1/2 particles ($N > 1$), there are two different methods to define the Husimi function

and the Wehrl entropy, corresponding to different choices of the coherent states $|\mathbf{n}\rangle$. In the first method, $\mathbf{n} \in S^2$ and $\{|\mathbf{n}\rangle\}$ are $SU(2)$ coherent states, which are multi-particle states with certain quantum numbers of the N -particle total spin and its component along the direction \mathbf{n} [13]. In the second method, $\{|\mathbf{n}\rangle\}$ are chosen to be the $SU(2)^{\otimes N}$ coherent states, which are the direct products of spin coherent states of each particle [11, 14]. Consequently, in the second method, the coherent-state label \mathbf{n} comprises N components, with each one being a 3D unit vector, *i.e.*, $\mathbf{n} \in S^{2 \otimes N}$.

In this work we investigate the Wehrl entropy of N spin-1/2 particles, which are defined via the second method shown above. The Wehrl entropy, as defined by this method, has been previously explored for two spin-1/2 particles in [11]. Here we consider the systems with arbitrary particle number N , and focus on the following two problems:

(1) *The statistical interpretation of the Husimi function and the Wehrl entropy.* Since the coherent states $\{|\mathbf{n}\rangle\}$ are not a group of orthonormal basis of the Hilbert space, the Husimi function cannot be directly interpreted as the probability distribution of the measurement outcomes of a certain observable, and thus the Wehrl entropy cannot be directly interpreted as the entropy corresponding to such a probability distribution. However, with the help of the Bayes theorem we prove that they can still be

* pengzhang@ruc.edu.cn

interpreted as an alternative well-defined probability distribution with clear physical meaning, and its entropy, respectively. In addition, under this interpretation the Wehrl entropy returns to the Gibbs entropy in the classical analogy.

(2) *The relationship between the Wehrl entropy and quantum entanglement, especially in the large- N systems.* It can be straightforwardly proven (Appendix C) that the Wehrl entropy of our system is invariant under local unitary transformations, and thus takes the same value $\Lambda_L N \equiv [\ln(2\pi) + 1/2]N$ for all the completely separable pure states. In 2003, A. Sugita [14] conjectured that the Wehrl entropy of all entangled states, as defined as above, are larger than that of the completely separable pure states. Based on the definition of the corresponding Husimi function, A. Sugita [14] also proposed that for many-body pure states the delocalization of the Husimi function, which can be measured by the Wehrl entropy, reflect the complexity of quantum entanglement (entanglement complexity). However, to our knowledge, the Wehrl entropy of specific entangled states of many-body systems (with particle number being larger than 3) has not been calculated in previous researches. As a result, the connection between the Wehrl entropy and the entanglement complexity has not been examined and studied for specific examples of these many-body systems.

Therefore, in this work we numerically calculate the Wehrl entropy for various pure states with respect to particle number $2 \leq N \leq 20$. The Wehrl entropy obtained by our calculation for the entangled pure states are all higher than that for the completely separable pure states, supporting the above conjecture of A. Sugita [14]. Furthermore, our numerical results indicate that in the large- N ($N \gtrsim 10$) cases the Wehrl entropy per particle of highly chaotic entangled states (*e.g.*, $2^{-N/2} \sum_{s_1, s_2, \dots, s_N = \uparrow, \downarrow} |s_1, s_2, \dots, s_N\rangle e^{-i\phi_{s_1, s_2, \dots, s_N}}$, with $\phi_{s_1, s_2, \dots, s_N}$ being independent random phases) are significantly larger than those of very regular entangled states, such as the Greenberger–Horne–Zeilinger (GHZ) state.

Our results yield that the Wehrl entropy does reflect the entanglement complexity of many-body pure states. In particular, the Wehrl entropy per particle can be used as a quantitative description of this entanglement complexity. Moreover, unlike other quantities used to evaluate this complexity, such as the degree of entanglement between a subsystem and the other particles, the Wehrl entropy per particle does not necessitate the division of the total system into two subsystems.

Furthermore, our numerical results suggest that many-body pure states can be categorized into three types, each exhibiting distinct behaviors of Wehrl entropy per particle as N approaches infinity, and differing in entanglement complexity.

The results of this work are helpful for the studies of the areas with entanglement complexity being very important, such as quantum many-body dynamics, chaos and thermalization, spin liquids, and quantum computation, as well as the deep understanding of Husimi func-

tion and Wehrl entropy.

The the statistical interpretation we developed for the Wehrl entropy is not used in the discussions for the relationship between the Wehrl entropy and quantum entanglement. Thus, the readers who are interested in the latter problem can skip the discussion for the former (*i.e.*, Sec. III).

The remainder of this paper is organized as follows. In Sec. II we introduce the definitions of the Husimi function and Wehrl entropy of N spin-1/2 particles. The statistical interpretation of the Wehrl entropy is given in Sec. III, and we briefly outline some properties of the Wehrl entropy in Sec. IV. In Sec. V we investigate the relationship between the Wehrl entropy and quantum entanglement. Sec. VI contains a summary and some discussions. In the appendices we illustrate more properties of the Wehrl entropy, as well as some details of our calculations.

II. DEFINITIONS OF THE HUSIMI FUNCTION AND WEHRL ENTROPY

We consider N spin-1/2 particles $1, \dots, N$. An $SU(2)^{\otimes N}$ spin coherent state is defined as a direct product of the spin coherent state of each particle:

$$|\mathbf{n}\rangle \equiv |\mathbf{n}_1\rangle_1 \otimes |\mathbf{n}_2\rangle_2 \otimes \dots \otimes |\mathbf{n}_N\rangle_N, \quad (1)$$

with

$$\mathbf{n} \equiv (\mathbf{n}_1, \mathbf{n}_2, \dots, \mathbf{n}_N) \in S^{2\otimes N}. \quad (2)$$

Here $\mathbf{n}_j \in S^2$ ($j = 1, \dots, N$) is a 3D unit vector, or the position vector of a point on the unit sphere (Bloch sphere) S^2 , and can be expressed as $\mathbf{n}_j = (\sin \theta_j \cos \phi_j, \sin \theta_j \sin \phi_j, \cos \theta_j)$, with $\theta_j \in [0, \pi]$, $\phi_j \in [0, 2\pi]$. Additionally, $S^{2\otimes N}$ is the Cartesian product of N unit spheres. Moreover, $|\mathbf{n}_j\rangle_j$ is the spin-coherent state of particle j with respect to the direction \mathbf{n}_j , which satisfies

$$\left[\hat{\sigma}^{(j)} \cdot \mathbf{n}_j \right] |\mathbf{n}_j\rangle_j = |\mathbf{n}_j\rangle_j, \quad (3)$$

where $\hat{\sigma}^{(j)} = (\hat{\sigma}_x^{(j)}, \hat{\sigma}_y^{(j)}, \hat{\sigma}_z^{(j)})$, with $\hat{\sigma}_{x,y,z}^{(j)}$ being the Pauli matrixes of the particle j ($j = 1, \dots, N$). The spin coherent states $\{|\mathbf{n}\rangle\}$ satisfy

$$\frac{1}{(2\pi)^N} \int d\mathbf{n} |\mathbf{n}\rangle \langle \mathbf{n}| = 1, \quad (4)$$

with

$$\int d\mathbf{n} = \prod_{j=1}^N \int_0^\pi \sin \theta_j d\theta_j \int_0^{2\pi} d\phi_j. \quad (5)$$

The Husimi function $P_H(\hat{\rho}; \mathbf{n})$ of this system is defined as

$$P_H(\hat{\rho}; \mathbf{n}) \equiv \frac{1}{(2\pi)^N} \langle \mathbf{n} | \hat{\rho} | \mathbf{n} \rangle, \quad (6)$$

copy	random unit vector	outcome of the measurement of $\hat{\sigma} \cdot \mathbf{u}$
$c^{(1)}$	$\mathbf{u}^{(1)}$	+1
$c^{(2)}$	$\mathbf{u}^{(2)}$	-1
$c^{(3)}$	$\mathbf{u}^{(3)}$	+1
$c^{(4)}$	$\mathbf{u}^{(4)}$	+1
$c^{(5)}$	$\mathbf{u}^{(5)}$	-1
\vdots	\vdots	\vdots

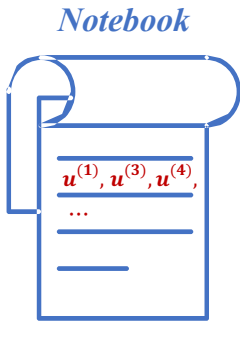


FIG. 1. A schematic illustration of the thought experiment of Sec. III for a single spin-1/2 particle. As shown in the table, in the η -th step ($\eta = 1, 2, \dots, m$), the experimenter measures the observable $\hat{\sigma} \cdot \mathbf{u}^{(\eta)}$ for the copy η . If and only if the outcome is +1, then the experimenter notes down the direction $\mathbf{u}^{(\eta)}$ in the notebook. In the case of this figure the outcome of the measurements 1, 3, 4, ... are +1, and thus the directions $\mathbf{u}^{(1,3,4,\dots)}$ are noted down in the notebook.

with $\hat{\rho}$ being the density operator of the N -body quantum state, describing the quantum state of all these particles. It is clear that $P_H(\hat{\rho}; \mathbf{n}) \geq 0$ for all \mathbf{n} , and

$$\int d\mathbf{n} P_H(\hat{\rho}; \mathbf{n}) = 1. \quad (7)$$

Notice that each Husimi function $P_H(\hat{\rho}; \mathbf{n})$ corresponds to a unique N -body state $\hat{\rho}$. Namely, if $\hat{\rho} \neq \hat{\rho}'$, then there definitely exists $\mathbf{n} \in S^{2\otimes N}$, which satisfies $P_H(\hat{\rho}; \mathbf{n}) \neq P_H(\hat{\rho}'; \mathbf{n})$.

Furthermore, the Wehrl entropy of these N spin-1/2 particles is defined as the entropy corresponding to the Husimi function:

$$S_W(\hat{\rho}) \equiv - \int P_H(\hat{\rho}; \mathbf{n}) \ln [P_H(\hat{\rho}; \mathbf{n})] d\mathbf{n}. \quad (8)$$

Clearly, the Wehrl entropy is a functional of the quantum state $\hat{\rho}$.

III. STATISTICAL INTERPRETATION OF THE HUSIMI FUNCTION AND THE WEHRL ENTROPY

In this section we demonstrate the statistical interpretation of the Husimi function and the Wehrl entropy. As mentioned before, the results in this section is not used in the subsequent sections. Therefore, the readers who are interested in the relation between the Wehrl entropy and quantum entanglement can skip this section and directly go to Sec. IV.

Since the coherent states $|\mathbf{n}\rangle$ and $|\mathbf{n}'\rangle$ defined above are not orthogonal if $\langle \mathbf{n}'_j | \mathbf{n}_j \rangle \neq 0$ for all $j = 1, \dots, N$, these states are not eigen-states of the same observable. Consequently, the Husimi function $P_H(\hat{\rho}; \mathbf{n})$ cannot be interpreted as the probability distribution of the outcome

of a measurement for any specific observable. Hence, the Wehrl entropy cannot be directly interpreted as the entropy of such a probability distribution.

Here we provide a statistical interpretation for the Husimi function and the Wehrl entropy. We will demonstrate that they can still be interpreted as a certain well-defined probability distribution with a clear physical meaning, and the corresponding entropy, respectively.

We begin from the single-particle case ($N = 1$). Consider the following thought experiment: Assume there are m copies $c^{(1)}, c^{(2)}, \dots, c^{(m)}$ of the spin-1/2 particle, with each one being in the same state $\hat{\rho}$. In addition, the experimenter generates m independent random unit vectors $\mathbf{u}^{(1)}, \mathbf{u}^{(2)}, \dots, \mathbf{u}^{(m)}$ from the unit sphere S^2 . Explicitly, the probability densities of these vectors in S^2 are all $1/(4\pi)$, and are independent of each other. Then the experimenter performs the following m steps: In the η -th step ($\eta = 1, \dots, m$), the experimenter measures the Pauli operator vector $\hat{\sigma}$ along the direction $\mathbf{u}^{(\eta)}$ (i.e., the observable $\hat{\sigma} \cdot \mathbf{u}^{(\eta)}$) for the copy $c^{(\eta)}$. If and only if the outcome of this measurement is +1, the experimenter notes down the direction $\mathbf{u}^{(\eta)}$ in a notebook. In Fig. 1 we schematically illustrate these m steps.

We consider the cases where m is very large, and assume that when all these m steps are finished, there are D directions noted down in the notebook. Then, the following question arises:

Question: What is the distribution of the directions noted down in the notebook? In another word, for a given direction $\mathbf{n} \in S^2$, how many directions, among the D ones in the notebook, are in a small solid angle $\Delta\Omega$ around \mathbf{n} ?

This question can be answered as follows:

Answer: Denote the answer to the above question (i.e., the number of directions in the region described above) as $\mathcal{N}(\mathbf{n})$. Since a direction can be noted down in the notebook if and only if the outcome of the corresponding measurement is +1, the answer to the above question can be expressed as:

$$\mathcal{N}(\mathbf{n}) = D\mathcal{P}(\mathbf{n} | +1) \Delta\Omega. \quad (9)$$

Here $\mathcal{P}(\mathbf{n} | +1)$ is a *conditional probability density*, i.e., the probability density of a randomly-chosen direction being \mathbf{n} , under the condition that the outcome of the measurement of the $\hat{\sigma}$ -operator along that direction is +1.

Moreover, according to Bayes' theorem, we have

$$\mathcal{P}(\mathbf{n} | +1) = \frac{\mathcal{P}(+1 | \mathbf{n})}{\mathcal{P}(+1)} \mathcal{P}(\mathbf{n}). \quad (10)$$

Here $\mathcal{P}(\mathbf{n}) = 1/(4\pi)$ is the probability density of a randomly-chosen direction being \mathbf{n} , $\mathcal{P}(+1 | \mathbf{n})$ is the probability that outcome of the measurement of the $\hat{\sigma}$ -operator along this random-chosen direction is +1 and can be expressed as

$$\mathcal{P}(+1 | \mathbf{n}) = \langle \mathbf{n} | \hat{\rho} | \mathbf{n} \rangle, \quad (11)$$

and $\mathcal{P}(+1) = \int d\mathbf{n}' \mathcal{P}(+1|\mathbf{n}') \mathcal{P}(\mathbf{n}')$.

Since both $\mathcal{P}(\mathbf{n})$ and $\mathcal{P}(+1)$ are independent of \mathbf{n} , Eqs. (10, 11) yield that $\mathcal{P}(\mathbf{n}|+1) = Z\langle \mathbf{n}|\hat{\rho}|\mathbf{n}\rangle$, with the constant Z being determined by the normalization condition $\int d\mathbf{n} \mathcal{P}(\mathbf{n}|+1) = 1$. Direct calculation gives $Z = 1/(2\pi)$. Therefore, we finally obtain $\mathcal{P}(\mathbf{n}|+1) = \langle \mathbf{n}|\hat{\rho}|\mathbf{n}\rangle/(2\pi)$, or

$$\mathcal{P}(\mathbf{n}|+1) = P_H(\hat{\rho}; \mathbf{n}). \quad (12)$$

Substituting this result into Eq. (9), we find that the amount of the noted-down directions in the small solid angle $\Delta\Omega$ among \mathbf{n} is:

$$\mathcal{N}(\mathbf{n}) = DP_H(\hat{\rho}; \mathbf{n})\Delta\Omega. \quad (13)$$

That is the answer to the question.

From the above discussion, we know that the Husimi function $P_H(\hat{\rho}; \mathbf{n})$ can be interpreted as the conditional probability density $\mathcal{P}(\mathbf{n}|+1)$. Moreover, in the above thought experiment with $m \rightarrow \infty$, we can consider the directions noted down in the notebook as an ensemble of directions in S^2 , and the probability distribution corresponding to this ensemble is just $P_H(\hat{\rho}; \mathbf{n})$.

The above discussions can be straightforwardly generalized to the multi-particle ($N > 1$) cases. In the thought experiment of these cases, each copy $c^{(\eta)}$ ($\eta = 1, \dots, m$) includes N particles, and every copy has the same N -body density operator $\hat{\rho}$. In addition, each $\mathbf{u}^{(\eta)}$ ($\eta = 1, \dots, m$) is randomly selected from $S^{2\otimes N}$, and includes N component with each one being in S^2 , *i.e.*, $\mathbf{u}^{(\eta)} \equiv (\mathbf{u}_1^{(\eta)}, \dots, \mathbf{u}_N^{(\eta)})$ with $\mathbf{u}_j^{(\eta)} \in S^2$ ($j = 1, \dots, N$). As before, the thought experiment includes m steps of measurement and noting. Nevertheless, now in the η -th step ($\eta = 1, \dots, m$), the experimenter needs to measure N observables, *i.e.*, measure the value of $\hat{\sigma} \cdot \mathbf{u}_j^{(\eta)}$ of the j -th particle of the copy $c^{(\eta)}$, for all $j = 1, \dots, N$. The experimenter notes down $\mathbf{u}^{(\eta)}$ in the notebook if and only if the outcomes of these N measurements are all +1.

As in the single-particle case, here we can still prove the relation of Eq. (12), while now $\mathbf{n} \equiv (\mathbf{n}_1, \dots, \mathbf{n}_N) \in S^{2\otimes N}$, with $\mathbf{n}_j \in S^2$ ($j = 1, \dots, N$). Therefore, for arbitrary particle number N , the Husimi function $P_H(\hat{\rho}; \mathbf{n})$ can always be interpreted as $\mathcal{P}(\mathbf{n}|+1)$, *i.e.*, the probability density of a randomly-chosen element of $S^{2\otimes N}$ being \mathbf{n} , under the condition that the outcomes of the measurements of $\hat{\sigma} \cdot \mathbf{n}_j$ of the particle j for each particle j ($j = 1, \dots, N$) are all +1. Clearly, it is also the distribution of the \mathbf{u} -vecotrs noted down in the thought experiment in the limit $m \rightarrow \infty$.

Furthermore, according to the above statistical interpretation of the Husimi function $P_H(\hat{\rho}; \mathbf{n})$, the Wehrl entropy can be interpreted as the entropy corresponding to the conditional probability density $\mathcal{P}(\mathbf{n}|+1)$ of our system, or the entropy corresponding to the distribution of the \mathbf{u} -vecotrs noted down in the thought experiment, in the limit that there are infinity copies.

So far we have obtained the statistical interoperation of the Husimi function and Wehrl entropy of the of N

quantum spin-1/2 particles. In Appendies A and B, we explore the classical correspondence of the above interpretation of the Wehrl entropy of spin-1/2 particles. Precisely speaking, spin-1/2 particles constitute a pure quantum system and do not have exact classical correspondences. Nevertheless, as described in Appendix A, precessing symmetric spinning tops can be viewed as a classical analogy of spin-1/2 particles. By calculating the related probabilities, we demonstrate that in this analogy, that in this analogy the Wehrl entropy of N quantum spin-1/2 particles corresponds the Gibbs entropy of N such classical tops.

IV. PROPERTIES OF THE WEHRL ENTROPY

In Appendix C we present and prove some properties of the Wehrl entropy and the Husimi function of N spin-1/2 particles. Here we introduce two ones of them, which will be utilized in the subsequent sections.

Property 1: For all N -particle density operators $\hat{\rho}$, the Wehrl entropy per particle (*i.e.*, S_W/N) satisfies

$$\frac{S_W(\hat{\rho})}{N} \leq \Lambda_U, \quad (14)$$

with

$$\Lambda_U \equiv \ln(4\pi) \approx 2.5310. \quad (15)$$

The equality in Eq. (14) is satisfied when the system is in the state $\hat{\rho} = \bigotimes_{j=1}^N (\hat{I}_j/2)$, where \hat{I}_j ($j = 1, \dots, N$) is the identity operator for particle j . This state is commonly referred to as the ‘‘maximum mixed state’’.

Property 2: The Wehrl entropy $S_W(\hat{\rho})$ is invariant under any local unitary transformation. Explicitly, if $\hat{\rho}' = U\hat{\rho}U^\dagger$ where $U = \bigotimes_{j=1}^N U_j$ and U_j ($j = 1, \dots, N$) is a unitary transformation acting on particle j , then $S_W(\hat{\rho}) = S_W(\hat{\rho}')$. This property implies that the Wehrl entropy is strongly related to quantum entanglement.

V. WEHRL ENTROPY AND ENTANGLEMENT

In this section we focus on the Wehrl entropy of N -body pure states, *i.e.*, $S_W(|\psi\rangle\langle\psi|)$, and investigate the relationship between the Wehrl entropy and quantum entanglement.

A. Wehrl Entropy of Completely Separable Pure States

We first consider the cases where $|\psi\rangle$ is a N -body completely separable pure state, *i.e.*, a direct product of pure states of each particle. Since the spin of each particle is 1/2, such a state is definitely an $S^{2\otimes N}$ spin-coherent state $|\mathbf{n}\rangle$ defined in Eq. (1).

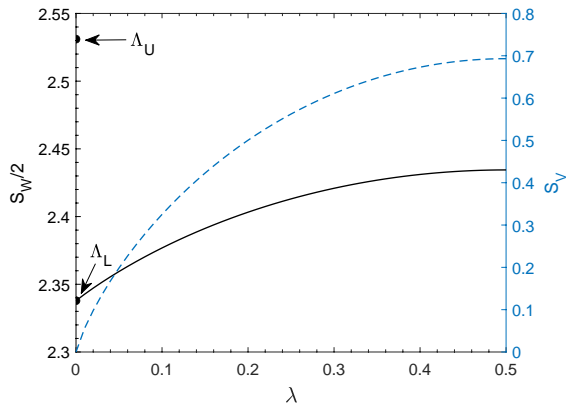


FIG. 2. The Wehrl entropy per particle of a two-body pure state $|\psi\rangle$ (black solid line) and the degree of entanglement $S_V(|\psi\rangle)$ (blue dashed line), as a functions of the parameter λ defined in Sec. VB. We also indicate the Wehrl entropy per particle of the completely separable pure state and maximum mixed state, *i.e.*, Λ_U and Λ_L .

As shown in the above section, $S_W(\hat{\rho})$ is invariant under any local unitary transformation. On the other hand, every two completely separable states can be related via a local unitary transformation. Therefore, all the completely separable states have the same Wehrl entropy. Explicitly, the direct calculations yield that

$$\frac{S_W(|\mathbf{n}\rangle\langle\mathbf{n}|)}{N} = \Lambda_L, \quad \forall \mathbf{n} \in S^{2^{\otimes N}}, \quad (16)$$

with

$$\Lambda_L \equiv \frac{1}{2} + \ln(2\pi) \approx 2.3379. \quad (17)$$

B. Wehrl Entropy of Two-Body Entangled States

Using the Schmidt-decomposition technique, one can prove that each pure state $|\psi\rangle$ of two particles 1 and 2 can always be written as $|\psi\rangle = U_1 \otimes U_2 |\varphi\rangle$, where U_j ($j = 1, 2$) is a unitary transformation acting on particle j , and

$$|\varphi\rangle = \sqrt{1-\lambda} |\uparrow\rangle_1 |\uparrow\rangle_2 + \sqrt{\lambda} |\downarrow\rangle_1 |\downarrow\rangle_2. \quad (18)$$

Here $\lambda \in [0, 1/2]$ is the smaller one of the two eigenvalues of the reduced density operator of particle 1, and $|\uparrow\rangle_j$ ($|\downarrow\rangle_j$) ($j = 1, 2$) is the eigen-state of $\hat{\sigma}_z^{(j)}$ with eigenvalue $+1$ (-1). Notice that the degree of entanglement of state $|\psi\rangle$ is characterized by the von Neuman entropy of $\hat{\rho}_1$, *i.e.*, $S_V(|\psi\rangle\langle\psi|) \equiv -\lambda \ln \lambda - (1-\lambda) \ln(1-\lambda)$. For instance, $|\psi\rangle$ is a separable state when $\lambda = 0$ ($S_V = 0$), and is a maximum entanglement state (Bell state) when $\lambda = 1/2$ ($S_V = \ln 2$).

As demonstrated in Sec. IV, the Wehrl entropy is invariable under local transformations. Due to this fact,

we have $S_W(|\psi\rangle\langle\psi|) = S_W(|\varphi\rangle\langle\varphi|)$, and thus $S_W(|\psi\rangle\langle\psi|)$ is a function of the parameter λ . In Fig. 2 we illustrate the Wehrl entropy per particle $S_W(|\psi\rangle\langle\psi|)/N$ ($N = 2$) and the entanglement degree $S_V(|\psi\rangle\langle\psi|)$ as functions of λ . It is shown that $S_W(|\psi\rangle\langle\psi|)/N$ increases with λ or $S_V(|\psi\rangle\langle\psi|)$. Therefore, the Wehrl entropy of a two-body pure entangled state is larger than the one of a separable state, and for all two-body pure states, the maximum entangled states (*i.e.*, the Bell states) have the largest Wehrl entropy.

C. Wehrl Entropy of Multi-Particle Entangled States

Now we study the relationship between the Wehrl entropy and the entanglement of pure states of multi ($N \geq 3$) spin-1/2 particles. Unfortunately, even up to a local unitary transformation, one cannot express an arbitrary pure state of these particles in a simple form like Eq. (18), which has only one parameters. As a result, we cannot investigate the Wehrl entropy of every pure states, as done above for the two-particle systems. Alternatively, we numerically calculate the Wehrl entropy for the entangled states of some typical types.

We numerically calculate the Wehrl entropy for the following states (In the following the symbol $|s_1, s_2, \dots, s_N\rangle$ ($s_1, s_2, \dots, s_N = \uparrow, \downarrow$) indicates the completely separable pure state $|s_1\rangle_1 \otimes |s_2\rangle_2 \otimes \dots \otimes |s_N\rangle_N$):

- **GHZ state:**

$$|\text{GHZ}\rangle \equiv \frac{1}{\sqrt{2}} \left[|\uparrow, \uparrow, \dots, \uparrow\rangle + |\downarrow, \downarrow, \dots, \downarrow\rangle \right]. \quad (19)$$

- **W state:**

$$|\text{W}\rangle \equiv \frac{1}{\sqrt{N}} \left[|\downarrow, \uparrow, \uparrow, \dots, \uparrow\rangle + |\uparrow, \downarrow, \uparrow, \dots, \uparrow\rangle + \dots + |\uparrow, \uparrow, \dots, \uparrow, \downarrow\rangle \right]. \quad (20)$$

- **p-Bell state:** the product-Bell state which is only defined only for even N , *i.e.*,

$$|\text{p-Bell}\rangle \equiv \bigotimes_{j=1,3,\dots,N-1} (|\uparrow\rangle_j |\uparrow\rangle_{j+1} + |\downarrow\rangle_j |\downarrow\rangle_{j+1}) / \sqrt{2}. \quad (21)$$

- **R1-state:** the state with equal amplitude and random sign, *i.e.*,

$$|\text{R1}\rangle \equiv \frac{1}{\sqrt{2^N}} \sum_{s_1, s_2, \dots, s_N = \uparrow, \downarrow} (-1)^{\xi_{s_1, s_2, \dots, s_N}} |s_1, s_2, \dots, s_N\rangle, \quad (22)$$

where $\xi_{s_1, s_2, \dots, s_N}$ ($s_j = \uparrow, \downarrow; j = 1, \dots, N$) are 2^N independent random coefficients, with each one taking values 0 or 1 with equal probabilities.

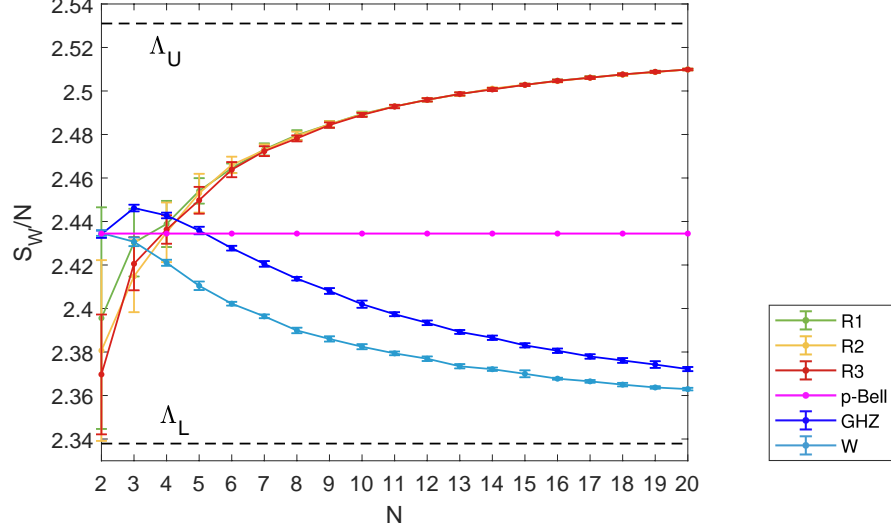


FIG. 3. The Wehrl entropy per particle of the states of types defined in Sec. V C. Here we show $\langle S_W/N \rangle$ for the GHZ and W states, and $\langle\langle S_W/N \rangle\rangle$ for the R1, R2 and R3 states. The error bars indicates δ_{MC} of the the GHZ and W states and δ_{tot} of the R1, R2 and R3 states. We also show the analytical result of the Wehrl entropy per particle of the p-Bell states without error bar. The Wehrl entropy per particle of the completely separable pure state and maximum mixed state, *i.e.*, Λ_U and Λ_L , respectively, are also shown as dashed lines. For more details, see Sec. V C.

- **R2-state:** the state with “equal amplitude and random phase”, *i.e.*,

$$|R2\rangle \equiv \frac{1}{\sqrt{2^N}} \sum_{s_1, s_2, \dots, s_N = \uparrow, \downarrow} |s_1, s_2, \dots, s_N\rangle e^{-i\phi_{s_1, s_2, \dots, s_N}}, \quad (23)$$

where $\phi_{s_1, s_2, \dots, s_N}$ ($s_j = \uparrow, \downarrow; j = 1, \dots, N$) are 2^N independent random angles, with each one taking values in the region $[0, 2\pi)$ with constant probabilistic density $1/(2\pi)$.

- **R3-state:** the “totally-random” state, *i.e.*,

$$|R3\rangle \equiv \frac{1}{Z} \sum_{s_1, s_2, \dots, s_N = \uparrow, \downarrow} C_{s_1, s_2, \dots, s_N} |s_1, s_2, \dots, s_N\rangle e^{-i\phi_{s_1, s_2, \dots, s_N}}, \quad (24)$$

where C_{s_1, s_2, \dots, s_N} and $\phi_{s_1, s_2, \dots, s_N}$ ($s_j = \uparrow, \downarrow; j = 1, \dots, N$) are 2^N independent random positive numbers and independent random angles, respectively. Explicitly, each C_{s_1, s_2, \dots, s_N} taking values in the region $[0, 1]$ with constant probabilistic density 1, and each $\phi_{s_1, s_2, \dots, s_N}$ taking values in the region $[0, 2\pi)$ with constant probabilistic density $1/(2\pi)$, and $Z = \sqrt{\sum_{s_1, s_2, \dots, s_N = \uparrow, \downarrow} C_{s_1, s_2, \dots, s_N}^2}$.

We analytically calculate the Wehrl entropy for the p-Bell states, and numerically calculate those for other

states by performing the integration in Eq. (8) using the Monte Carlo method, for $2 \leq N \leq 20$. Explicitly, for the GHZ and W states, we perform the integration for ten times for each particle number N , and then derive the average value $\langle S_W/N \rangle$ as well as the standard deviation δ_{MC} . For the R1, R2 and R3 states, for each N we first generate five samples of the random parameters in the definitions of these states (*i.e.*, the ξ -, C - and ϕ -parameters). For each state with respect to a certain sample, we calculate $\langle S_W/N \rangle$ and δ_{MC} as above. We further derive the average value and the standard deviation of $\langle S_W/N \rangle$ of these five states, which are denoted as $\langle\langle S_W/N \rangle\rangle$ and δ_{R} , respectively. Additionally, we define $\delta_{\text{tot}} \equiv \delta_{\text{R}} + \delta_{\text{MC}}^{\text{max}}$, where $\delta_{\text{MC}}^{\text{max}}$ is the maximum value of δ_{MC} these five states.

In Fig. 3 we show the Wehrl entropy per particle obtained from the above calculations as functions of N . Explicitly, we illustrate $\{\langle S_W/N \rangle, \delta_{\text{MC}}\}$ for the GHZ and W states, and illustrate $\{\langle\langle S_W/N \rangle\rangle, \delta_{\text{tot}}\}$ for the R1, R2 and R3 states. The analytical results of S_W/N for the p-Bell states is also shown in this figure.

In addition to the aforementioned states, we also calculate the Wehrl entropy of the time-dependent states $|\psi(t)\rangle$ governed by the time-dependent Schrödinger equation of some models listed in Appendix D.

From the these calculations, we obtain the following understandings for the Wehrl entropy of multi-particle entangled pure states:

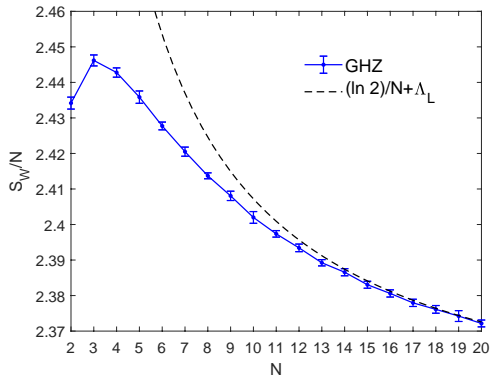


FIG. 4. **Solid line with error bars:** the Wehrl entropy per particle of the GHZ states, which are given by our numerical calculation (*i.e.*, the results shown in Fig. 3). **Dashed line:** $(\ln 2)/N + \Lambda_L$.

(a) The lower and upper bounds of Wehrl entropy

As shown in Fig. 3, the Wehrl entropy per particle of all the states of types (i-v) are larger than the one of the completely separable pure states, *i.e.*, Λ_L . The same is true for the Wehrl entropy per particle of we obtained for the states of Appendix D. These results consist with the conjecture of A. Sugita [14], which yields that for our system the Wehrl entropy takes the minimum value for the spin coherent states.

According to this conjecture, Λ_L is the lower bound of the Wehrl entropy per particle of all density operators. This result, together with the property shown in Eq. (14), further leads to

$$\Lambda_L \leq \frac{S_W(\hat{\rho})}{N} \leq \Lambda_U, \quad \text{for } \forall \hat{\rho}. \quad (25)$$

(b) Wehrl entropy and entanglement complexity of multi-particle pure states

As shown in Fig. 3, when the particle number N is large enough ($N \gtrsim 10$.) the Wehrl entropy per particle of the the R1, R2 or R3 states, which are almost same, are significantly larger than the ones of the GHZ or W states. On the other hand, we notice that there is big difference between the R1/R2/R3 states and the GHZ/W states: the former ones are very chaotic (complicated) while the latter ones are very regular (simple). Explicitly, the R1/R2/R3 states include 2^N terms with very random coefficients, while the GHZ or W states only include 2 or N terms with equal coefficients. Thus, the Wehrl entropy is larger when $|\psi\rangle$ is entangled more complicated. Moreover, since the Wehrl entropy is invariant under local unitary transformations (the property 2 of Sec. IV), for pure states it is only determined by the entanglement. Therefore, one can use the Wehrl entropy per particle as a quantitative description of the entan-

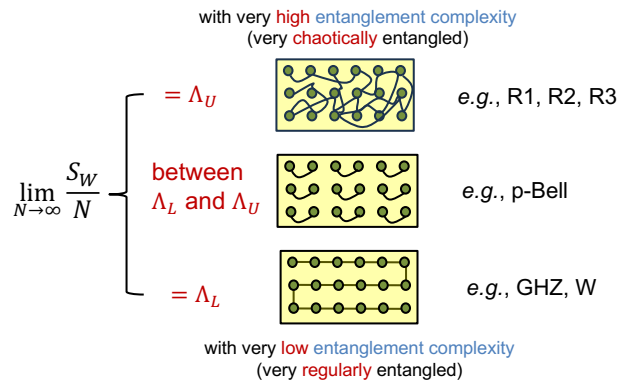


FIG. 5. The three types of behaviors of $\lim_{N \rightarrow \infty} S_W/N$ of many-body pure states. The yellow rectangles with connected discs are just schematic diagrams for the entanglement complexity of the states of each type. The detailed discussions are given in Sec. VC.

glement complexity of N -body pure states of spin-1/2 particles.

Furthermore, in the calculation of the Wehrl entropy, one does not require to divide the system into two subsystems. This is a big difference between the Wehrl entropy and some other descriptions of the entanglement complexity of a multi-particle system, *e.g.*, the entanglement entropy between a subsystem and the other particles.

As mentioned above, we calculate the Wehrl entropy of the time-dependent states $|\psi(t)\rangle$ of the models in Appendix D. Our results show that when $N \geq 10$ the Wehrl entropy per particle of all these states are below or equal to the ones of the R1/R2/R3 states.

(c) Behaviors of Wehrl entropy in the limit $N \rightarrow \infty$

Fig. 3 shows that when the particle number N is large, the Wehrl entropy per particle of the R1, R2 and R3 states increase with N , while the one of the ones of GHZ/W states decrease with N . We numerically fit the results of these states with $N \geq 16$ as functions of N , and find that within the error bar of the fitting, in the limit $N \rightarrow \infty$ the Wehrl entropy per particle of the R1/R2/R3 states and the ones of the GHZ/W states tend Λ_U and Λ_L , respectively. The details of the fitting results are shown in the footnote [16].

Due to these results, we conjecture that $\lim_{N \rightarrow \infty} S_W/N = \Lambda_L$ for the GHZ/W states, and $\lim_{N \rightarrow \infty} S_W/N = \Lambda_U$ for the R1/R2/R3 states. Moreover, in Appendix E we performs rough analysis which supports the above conjectures for the GHZ and R1/R2 states. Additionally, this analysis also show that for GHZ state we have $S_W(\hat{\rho})/N \approx (\ln 2)/N + \Lambda_L$ for the large- N cases. As shown in Fig. 4, this approximate expression agrees well with our numerical results when $N \gtrsim 16$. Moreover, it can be directly proved that the Wehrl entropy per particle of the p-Bell states is a

N -dependent constant (approximately 2.43) between Λ_L and Λ_N , as shown in Fig. 3.

Therefore, the multi-particle entangled pure states of our system can be classified into three types, according to the behaviors of S_W/N (Fig. 5), *i.e.*, the states with:

$$\lim_{N \rightarrow \infty} \frac{S_W}{N} = \Lambda_U \quad (\text{type I}),$$

$$\Lambda_L < \lim_{N \rightarrow \infty} \frac{S_W}{N} < \Lambda_U \quad (\text{type II}),$$

$$\lim_{N \rightarrow \infty} \frac{S_W}{N} = \Lambda_L \quad (\text{type III}).$$

Specifically, states of type I (*e.g.*, the R1/R2/R3 states) exhibit highly chaotic entanglement, resulting in such a high entanglement complexity that, for $N \rightarrow \infty$ the Wehrl entropy tends towards that of the maximum mixed state (*i.e.*, the upper bound of the Wehrl entropy for all density operators). In contrast, the states of type III (*e.g.*, the GHZ/W states) are entangled very regularly, so that for $N \rightarrow \infty$ the Wehrl entropy tends to the one of the completely separable pure states (*i.e.*, the lower bound of the Wehrl entropy for all density operators). The entanglement complexity of the states of the type II are between that of the above two types.

VI. SUMMARY AND DISCUSSION

In this work we present a statistical interpretation for the Wehrl entropy of N spin-1/2 particles, and evaluate the relation between the Wehrl entropy and entanglement of quantum pure states. The discussions for the statistical interpretation and the classical analogy can be generalized to other systems, including those with continuous variables, and maybe helpful for the understanding of chaotic behaviors in quantum systems.

Moreover, as shown above, the Wehrl entropy per particle can be used as a quantitative description for the entanglement complexity of multi-particle pure states, without dividing the total system into two or more subsystems, and thus would be helpful for the studies of related many-body problems.

We emphasize that the Wehrl entropy can describe the entanglement complexity only for the pure states. It would be very helpful if a description of this complexity of the multi-particle mixed states can be found.

ACKNOWLEDGMENTS

The authors thank Yingfei Gu, Dazhi Xu, Pengfei Zhang, Hui Zhai, Honggang Luo, Zhiyuan Xie, and Ninghua Tong for fruitful discussions. This work was supported by the National Key Research and Development Program of China (Grant No. 2022YFA1405300), and NSAF Grant No. U1930201.

Appendix A: Classical Correspondence of the Husimi Function and Wehrl Entropy

In this appendix we study the classical correspondence of the statistical interpretation of Husimi function and Wehrl entropy of spin-1/2 particles, which are given in Sec. III.

As in that section, we begin from the single-particle ($N = 1$) case. Precisely speaking, a spin-1/2 particle is a pure quantum system and does not have exact classical correspondence. Nevertheless, we can still find “classical analogies” for this kind of particle, *i.e.*, classical systems with dynamic equations being equivalent to the Heisenberg equations of a spin-1/2 particle.

In Fig 6(a) we present one example of such systems: a charged axial symmetric top precessing in a homogeneous magnetic field. Explicitly, the top is rapidly spinning along its symmetry axis with fixed angular speed ω , and the center-of-mass of this top is fixed in an inertial frame of reference. In addition, an electric charge Q is fixed on the edge of the top, forming an electric current during the spinning. Due to this current, the top gains a magnetic moment, and thus is subject to a force moment from the magnetic field. The precession of this top, *i.e.*, the changing of the the direction of the symmetry axis of the top in the inertial frame of reference, is caused by this force moment. During the precession, the unit vector \mathbf{w} along the symmetry axis of the top satisfies the dynamical equation

$$\frac{d\mathbf{w}}{dt} = C\mathbf{w} \times \mathbf{B}, \quad (\text{A1})$$

where \mathbf{B} is the magnetic field and $C = QR^2/(2I)$. Here R is the distance between the charge and the symmetric axis of the top, and I is the moment of inertia of the top along this axis. On the other hand, the Hamiltonian of a quantum spin-1/2 particle can always be written as (up to a constant) a linear combination of Pauli operators $\sigma_{x,y,z}$, *i.e.*, $H_S = \hbar \sum_{\alpha=x,y,z} f_\alpha \sigma_\alpha$. Thus, the corresponding Heisenberg equation is

$$\frac{d\hat{\sigma}_H}{dt} = -2\hat{\sigma}_H \times \mathbf{f}, \quad (\text{A2})$$

where $\hat{\sigma}_H = (\hat{\sigma}_{xH}, \hat{\sigma}_{yH}, \hat{\sigma}_{zH})$ is the time-dependent Pauli-operator vector in the Heisenberg picture, and $\mathbf{f} = (f_x, f_y, f_z)$. Clearly, this Heisenberg equation is equivalent to the dynamical equation (A1) of the above charged spinning top in a magnetic field $\mathbf{B} = -2\mathbf{f}/C$.

The above analysis reveals that the charged spinning top is a classical analogy of a quantum spin-1/2 particle. The direction vector $\mathbf{w} \equiv (w_x, w_y, w_z)$ of the top axis is just the classical analogy of the Pauli -operator vector $\hat{\sigma} \equiv (\hat{\sigma}_x, \hat{\sigma}_y, \hat{\sigma}_z)$ of the spin-1/2 particle. Furthermore, as shown in Appendix B, the classical dynamical equation (A1) of the top can be re-expressed as a Hamiltonian equation, and the phase space of this system is just the set of all possible direction vectors of the top axis, coinciding with the unit sphere S^2 . As a result, the state of

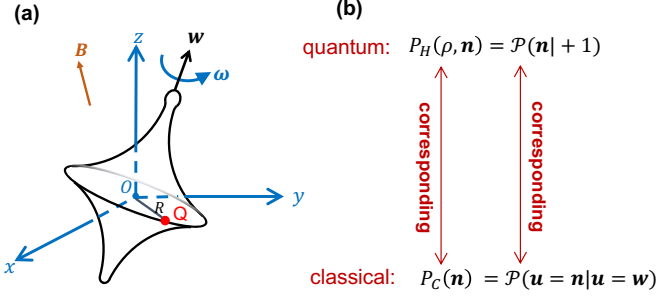


FIG. 6. **(a)**: A spinning charged top precessing in a homogeneous magnetic field, which is a classical analogy of a spin-1/2 particle. Here O is the center-of-mass of the top, and \mathbf{w} is the unit vector along the symmetry axis. Other details are introduced in Appendix A. **(b)**: The identities proven in Secs. III and Appendix A for the quantum and classical systems, respectively, and the quantum-classical correspondence of the related functions.

this classical top is described by the phase-space probability distribution $P_C(\mathbf{n})$ with $\mathbf{n} \in S^2$. Explicitly, $P_C(\mathbf{n})$ represents the probability density of the event that the symmetry axis of the top is along \mathbf{n} , *i.e.*, $\mathbf{w} = \mathbf{n}$.

In the discussion in Sec. III, which is for the spin-1/2 quantum particle, we introduced the conditional probability density $\mathcal{P}(\mathbf{n}|+1)$. Now let us consider the classical correspondence of $\mathcal{P}(\mathbf{n}|+1)$. As shown above, the classical correspondence of the $\hat{\sigma}$ -operator is the symmetry axis direction \mathbf{w} . Therefore, for a given direction $\mathbf{u} \in S^2$, the classical correspondence of the event $\hat{\sigma} \cdot \mathbf{u} = +1$ is the event $\mathbf{w} \cdot \mathbf{u} = 1$ or $\mathbf{u} = \mathbf{w}$. Therefore, the classical correspondence of $\mathcal{P}(\mathbf{n}|+1)$ is a conditional probability density $\mathcal{P}(\mathbf{u} = \mathbf{n}|\mathbf{u} = \mathbf{w})$, which is defined as the probability that a random direction \mathbf{u} being in a small solid angle $\Delta\Omega$ around the direction \mathbf{n} , under the condition that $\mathbf{u} = \mathbf{w}$, is $\mathcal{P}(\mathbf{u} = \mathbf{n}|\mathbf{u} = \mathbf{w}) \Delta\Omega$. Clearly, $\mathcal{P}(\mathbf{u} = \mathbf{n}|\mathbf{u} = \mathbf{w})$ can in principle be measured via a “classical version” of the thought experiment in Sec. III [17].

Furthermore, for a charged spinning top with phase-space distribution function $P_C(\mathbf{n})$, the conditional probability density $\mathcal{P}(\mathbf{u} = \mathbf{n}|\mathbf{u} = \mathbf{w})$ can be calculated via Bayes’ theorem as:

$$\mathcal{P}(\mathbf{u} = \mathbf{n}|\mathbf{u} = \mathbf{w}) = \frac{\mathcal{P}(\mathbf{u} = \mathbf{w}|\mathbf{u} = \mathbf{n})}{\mathcal{P}(\mathbf{u} = \mathbf{w})} \mathcal{P}(\mathbf{u} = \mathbf{n}), \quad (\text{A3})$$

where $\mathcal{P}(\mathbf{u} = \mathbf{n}) = 1/(4\pi)$ is the probability density of the random vector \mathbf{u} being \mathbf{n} , $\mathcal{P}(\mathbf{u} = \mathbf{w}|\mathbf{u} = \mathbf{n})$ is the probability density of $\mathbf{u} = \mathbf{w}$ under the condition that $\mathbf{u} = \mathbf{n}$, and $\mathcal{P}(\mathbf{u} = \mathbf{w}) = \int d\mathbf{n}' \mathcal{P}(\mathbf{u} = \mathbf{w}|\mathbf{u} = \mathbf{n}') \mathcal{P}(\mathbf{u} = \mathbf{n}')$. Because $\mathcal{P}(\mathbf{u} = \mathbf{n})$ and $\mathcal{P}(\mathbf{u} = \mathbf{w})$ are all independent of \mathbf{n} , Eq. (A3) yields

$$\mathcal{P}(\mathbf{u} = \mathbf{n}|\mathbf{u} = \mathbf{w}) = \xi \mathcal{P}(\mathbf{u} = \mathbf{w}|\mathbf{u} = \mathbf{n}), \quad (\text{A4})$$

where ξ is the normalization factor determined by the condition $\int d\mathbf{n} \mathcal{P}(\mathbf{u} = \mathbf{n}|\mathbf{u} = \mathbf{w}) = 1$. Furthermore, we

have

$$\begin{aligned} \mathcal{P}(\mathbf{u} = \mathbf{w}|\mathbf{u} = \mathbf{n}) &= \mathcal{P}(\mathbf{w} = \mathbf{n}|\mathbf{u} = \mathbf{n}) \\ &= P_C(\mathbf{n}), \end{aligned} \quad (\text{A5})$$

where the second equality is due to the fact that $\mathcal{P}(\mathbf{w} = \mathbf{n}|\mathbf{u} = \mathbf{n})$ is just the probability density of $\mathbf{w} = \mathbf{n}$, *i.e.*, $P_C(\mathbf{n})$. Substituting Eq. (A5) into Eq. (A4), and using the normalization condition, we finally obtain

$$\mathcal{P}(\mathbf{u} = \mathbf{n}|\mathbf{u} = \mathbf{w}) = P_C(\mathbf{n}). \quad (\text{A6})$$

As shown above, in our quantum-classical analogy the classical correspondence of $\mathcal{P}(\mathbf{n}|+1)$ is a conditional probability density $\mathcal{P}(\mathbf{u} = \mathbf{n}|\mathbf{u} = \mathbf{w})$. Additionally, as shown in Sec. III, in the quantum case we have $\mathcal{P}(\mathbf{n}|+1) = P_H(\hat{\rho}; \mathbf{n})$. Moreover, Eq. (A6) show that in the classical side we have $\mathcal{P}(\mathbf{u} = \mathbf{n}|\mathbf{u} = \mathbf{w}) = P_C(\mathbf{n})$. Therefore, the classical correspondence of the Husimi function $P_H(\hat{\rho}; \mathbf{n})$ is the phase-probability distribution function $P_C(\mathbf{n})$ (Fig. 6(b)).

Using the above conclusion and the relationship between the Wehrl entropy and the Husimi function (*i.e.*, Eq. (8)), we further find that the classical analogy of the Wehrl entropy is $-\int P_C(\mathbf{n}) \ln [P_C(\mathbf{n})] d\mathbf{n}$. This is nothing but the Gibbs entropy of the spinning top because $P_C(\mathbf{n})$ is the phase-space probability distribution function of this top.

The above discussions can be directly generalized to the multi-particle cases with $N > 1$. The classical analogy of N spin-1/2 particles are N charged spinning tops, and the N -body phase space is the product $S^{2\otimes N}$ of the N spheres. Similar as above, one can find that the classical analogy of the Husimi function and Wehrl entropy of the N quantum particles are the probability distribution of the tops in this N -body phase space and the corresponding Gibbs entropy, respectively.

Appendix B: The Phase Space of a Charged Spinning Top

In this appendix we show that the phase space of the charged spinning top of Appendix A is just the unit sphere S^2 .

The canonical coordinate of this top can be chosen as the azimuth angle φ and the z -component w_z of the direction vector $\hat{\mathbf{w}}$ of the top axis (Fig. 6(a)). Then the Lagrangian of this system is given by

$$\begin{aligned} L_{\text{top}} &= C \left[B_z w_z + B_x \sqrt{1 - w_z^2} \cos \varphi + B_y \sqrt{1 - w_z^2} \sin \varphi \right] \\ &\quad + \dot{\varphi} w_z. \end{aligned} \quad (\text{B1})$$

It can be straightforwardly proven that the Lagrangian equaitons

$$\frac{d}{dt} \left(\frac{\partial L_{\text{top}}}{\partial \dot{\varphi}} \right) - \frac{\partial L_{\text{top}}}{\partial \varphi} = 0; \quad (\text{B2})$$

$$\frac{d}{dt} \left(\frac{\partial L_{\text{top}}}{\partial \dot{w}_z} \right) - \frac{\partial L_{\text{top}}}{\partial w_z} = 0, \quad (\text{B3})$$

are equivalent to the classical dynamical equation (A1) of this top, and the x and y components $w_{x,y}$ of the direction vector $\hat{\mathbf{w}}$ are functions of the canonical coordinates, *i.e.*, $w_x = \sqrt{1 - w_z^2} \cos \varphi$ and $w_y = \sqrt{1 - w_z^2} \sin \varphi$.

Moreover, the canonical momentums p_φ and p_w of our system are canonical coordinates

$$p_\varphi = \frac{\partial L_{\text{top}}}{\partial \dot{\varphi}} = w_z; \quad (\text{B4})$$

$$p_w = \frac{\partial L_{\text{top}}}{\partial \dot{w}_z} = 0. \quad (\text{B5})$$

Therefore, although there are two canonical coordinates, the phase space of our system two-dimensional, rather than four-dimensional. Explicitly, this phase space is the space of (φ, w_z) , with $\varphi \in [0, 2\pi)$ and $w_z \in [-1, 1]$. In addition, the measurement (area element) of this phase space is $d\varphi dw_z$. It is clear that this phase space is equivalent to the unit sphere S^2 with azimuth angle being φ and polar angle being $\theta \equiv \arccos w_z = \arccos p_\varphi$, *i.e.*, the set of all possible direction vectors $\hat{\mathbf{w}}$. Moreover, the measurement $d\varphi dw_z$ just equals to $\sin \theta d\theta d\varphi$, *i.e.*, the area element of the S^2 sphere.

In the end of this appendix, for reference, we provide the Hamiltonian of this charged spinning top:

$$\begin{aligned} H_{\text{top}} &= -C \left[B_z p_\varphi + B_x \sqrt{1 - p_\varphi^2} \cos \varphi + B_y \sqrt{1 - p_\varphi^2} \sin \varphi \right]. \end{aligned} \quad (\text{B6})$$

Appendix C: Properties of the Wehrl Entropy and Husimi Function

In this appendix, we demonstrate and prove some properties of the Husimi function and the Wehrl entropy of N spin-1/2 particles, including but not limited to the two ones presented in Sec. IV.

1. Invariance of the Wehrl Entropy Under Local Unitary Transformations

We first prove the ‘‘property 2’’ of Sec. IV, *i.e.*, the Wehrl entropy $S_W(\hat{\rho})$ is invariable under any local unitary transformation. Explicitly, if two density operators $\hat{\rho}$ and $\hat{\rho}'$ satisfy $\hat{\rho}' = U \hat{\rho} U^\dagger$, where $U = \bigotimes_{j=1}^N U_j$ and U_j ($j = 1, \dots, N$) is a unitary transformation of particle j , then we have $S_W(\hat{\rho}) = S_W(\hat{\rho}')$.

This property can be proved directly with the definitions of the Husimi function and Wehrl entropy. We first consider the case with $N = 1$. In this case the Wehrl entropy of $\hat{\rho}'$ is

$$S_W(\hat{\rho}') = - \int P_H(\hat{\rho}'; \mathbf{n}) \ln \left[P_H(\hat{\rho}'; \mathbf{n}) \right] d\mathbf{n}. \quad (\text{C1})$$

On the other hand, we have

$$\begin{aligned} P_H(\hat{\rho}'; \mathbf{n}) &= \frac{1}{(2\pi)^N} \langle \mathbf{n} | U \hat{\rho} U^\dagger | \mathbf{n} \rangle \\ &= \frac{1}{(2\pi)^N} \langle \mathbf{n}' | \hat{\rho} | \mathbf{n}' \rangle \\ &= P_H(\hat{\rho}; \mathbf{n}'). \end{aligned} \quad (\text{C2})$$

Here the direction \mathbf{n}' is a function of \mathbf{n} , and satisfies

$$\hat{\sigma} \cdot \mathbf{n}' = U^\dagger \hat{\sigma} \cdot \mathbf{n} U. \quad (\text{C3})$$

Therefore, we have

$$S_W(\hat{\rho}') = - \int P_H(\hat{\rho}; \mathbf{n}') \ln \left[P_H(\hat{\rho}; \mathbf{n}') \right] d\mathbf{n}. \quad (\text{C4})$$

Furthermore, the relation (C3) between the unit vectors \mathbf{n}' and \mathbf{n} can be written as $\mathbf{n}' = R_U \mathbf{n}$, with R_U the rotation on the Bloch sphere, which corresponds to the unitary transformation U . The results yields that $d\mathbf{n} = d\mathbf{n}'$, *i.e.*, the Jacobi determinant corresponding to the transformation $\mathbf{n} \rightarrow \mathbf{n}'$ is unit. Combining this fact and Eq. (C4), we obtain

$$\begin{aligned} S_W(\hat{\rho}') &= - \int P_H(\hat{\rho}; \mathbf{n}') \ln \left[P_H(\hat{\rho}; \mathbf{n}') \right] d\mathbf{n}' \\ &= S_W(\hat{\rho}). \end{aligned} \quad (\text{C5})$$

So far we have proved this property for the single particle case. The proof for arbitrary particle number N can be done with the same approach.

2. The Relation Between the Husimi Functions of the Total System and Subsystems

If the density operator of N spin-1/2 particles is $\hat{\rho}$, then the reduced density operator $\hat{\rho}_{\text{sub}}$ of a subsystem including M particles i_1, i_2, \dots, i_M is

$$\hat{\rho}_{\text{sub}} = \text{Tr}_{i \notin \{i_1, i_2, \dots, i_M\}} \hat{\rho}. \quad (\text{C6})$$

Here $\text{Tr}_{i \notin \{i_1, i_2, \dots, i_M\}}$ means tracing over the particles except i_1, i_2, \dots, i_M . The Husimi function $P_H(\hat{\rho}_{\text{sub}}; \mathbf{n}_{\text{sub}})$, with $\mathbf{n}_{\text{sub}} \equiv (\mathbf{n}_{i_1}, \mathbf{n}_{i_2}, \dots, \mathbf{n}_{i_M}) \in S^{2 \otimes M}$, is related to the Husimi function $P_H(\hat{\rho}; \mathbf{n})$ of all the N -particles via

$$P_H(\hat{\rho}_{\text{sub}}; \mathbf{n}_{\text{sub}}) = \int P_H(\hat{\rho}; \mathbf{n}) \prod_{i \notin \{i_1, i_2, \dots, i_M\}} d\mathbf{n}_i. \quad (\text{C7})$$

This can be proved directly with the definition of the Husimi function.

3. The Subadditivity, Monotonicity and Concavity of the Wehrl Entropy

The N spin-1/2 particles can be separated into two subsystems A and B , with A including particles

i_1, i_2, \dots, i_M and B including other particles. If the density operators of the N particles is $\hat{\rho}$, and the reduced operators of the subsystems A and B are $\hat{\rho}_A$ and $\hat{\rho}_B$, respectively, then we have

$$S_W(\hat{\rho}) \leq S_W(\hat{\rho}_A) + S_W(\hat{\rho}_B) = S_W(\hat{\rho}_A \otimes \hat{\rho}_B) \quad (\text{subadditivity}), \quad (\text{C8})$$

and

$$S_W(\hat{\rho}_A), S_W(\hat{\rho}_B) \leq S_W(\hat{\rho}) \quad (\text{monotonicity}). \quad (\text{C9})$$

Furthermore, if three N -body density operators $\hat{\rho}$, $\hat{\rho}^{(1)}$ and $\hat{\rho}^{(2)}$ satisfy $\hat{\rho} = p_1 \hat{\rho}^{(1)} + p_2 \hat{\rho}^{(2)}$, with $p_{1,2} > 0$ and $p_1 + p_2 = 1$, when we have

$$S_W(\hat{\rho}) \geq p_1 S_W(\hat{\rho}^{(1)}) + p_2 S_W(\hat{\rho}^{(2)}) \quad (\text{concavity}). \quad (\text{C10})$$

These results can be proved directly via Eq. (C7) and the methods used in Ref. [1] (subadditivity and concavity) and Ref. [7] (monotonicity).

Due to Eq. (C8), for every N -body state $\hat{\rho}$, we have

$$S_W(\hat{\rho}) \leq \sum_{j=1}^N S_W(\hat{\rho}_j), \quad (\text{C11})$$

with $\hat{\rho}_j$ ($j = 1, \dots, N$) being the reduced density operator of particle j . On the other hand, it can be directly proved that for a spin-1/2 particle, the Wehrl entropy is at most $\Lambda_U \equiv \ln(4\pi)$. Using this fact and Eq. (C11), we obtain the ‘‘property 1’’ of Sec. IV.

Appendix D: Dynamical Models

As mentioned in Sec. VC, we have calculated the Wehrl entropy of the states $|\psi(t)\rangle$ determined by the time-dependent Schrödinger equation with the following Hamiltonians.

(1): The Ising model with Hamiltonian

$$H_{\text{Ising}} \equiv - \left[\sum_{j=1}^{N-1} \sigma_z^{(j)} \sigma_z^{(j+1)} + \sigma_z^{(N)} \sigma_z^{(1)} \right]. \quad (\text{D1})$$

For this model we consider the cases with initial state

$$|\psi(t=0)\rangle = \bigotimes_{j=1}^N (|\uparrow\rangle_j + |\downarrow\rangle_j) / \sqrt{2}, \quad (\text{D2})$$

particle number $N = 5$, and evolution time $t \in [0, 40]$, as well as that with the same initial state and $2 \leq N \leq 14$, $t \in [30, 40]$.

(2): The XY model with Hamiltonian

$$H_{\text{XY}} \equiv - \left\{ \sum_{j=1}^{N-1} \left[\sigma_x^{(j)} \sigma_x^{(j+1)} + \sigma_y^{(j)} \sigma_y^{(j+1)} \right] + \sigma_x^{(N)} \sigma_x^{(1)} + \sigma_z^{(N)} \sigma_z^{(1)} \right\}. \quad (\text{D3})$$

The initial states, particle numbers, and evolution times of the cases we consider for this model are same as those of the above Ising model.

(3): The Ising model with both a transverse and a longitudinal field with Hamiltonian

$$H_{\text{TLI}} \equiv H_{\text{Ising}} - \sum_{j=1}^N \left[\sigma_y^{(j)} + \sigma_z^{(j)} \right], \quad (\text{D4})$$

with H_{Ising} being defined in Eq. (D1). The initial states, particle numbers, and evolution times of the cases we consider for this model are same as those of the above Ising model.

(4): The Ising model with both a transverse and a longitudinal field with Hamiltonian

$$H_{\text{TLI}} \equiv H_{\text{Ising}} - \sum_{j=1}^N \left[\sigma_x^{(j)} + g_z \sigma_z^{(j)} \right], \quad (\text{D5})$$

with H_{Ising} being defined in Eq. (D1) and $g_z = 0, 0.1, 0.5, 1, 2$. For this model we consider the cases with particle number $N = 6$, evolution time $t \in [0, 40]$ and the initial states being either the one of Eq. (D2) or $|\psi(t=0)\rangle = \bigotimes_{j=1}^N |\mathbf{u}_j\rangle_j$, where \mathbf{u}_j ($j = 1, \dots, N$) are random directions.

Appendix E: Behaviors of S_W/N for $N \rightarrow \infty$

In this appendix we provide two rough analysis, which imply that for the R1 and R2 states we have $\lim_{N \rightarrow \infty} S_W/N = \Lambda_U$, and for the GHZ states we have $\lim_{N \rightarrow \infty} S_W/N = \Lambda_L$ and $S_W/N \approx (\ln 2)/N + \Lambda_L$ in the large- N limit.

We first consider the GHZ states defined in Eq. (4). According to Eq. (6), the Husimi function of this state is given by

$$P_H(\mathbf{n}) = \frac{1}{2} \left\{ P_H^{(1)}(\mathbf{n}) + P_H^{(2)}(\mathbf{n}) + P_H^{(3)}(\mathbf{n}) + P_H^{(3)}(\mathbf{n})^* \right\}, \quad (\text{E1})$$

where $P_H^{(1)}(\mathbf{n})$ and $P_H^{(2)}(\mathbf{n})$ are the Husimi functions of the states $|\uparrow, \uparrow, \dots, \uparrow\rangle$ and $|\downarrow, \downarrow, \dots, \downarrow\rangle$, respectively, and

$$P_H^{(3)}(\mathbf{n}) = \frac{1}{(2\pi)^N} \langle \mathbf{n} | \uparrow, \uparrow, \dots, \uparrow \rangle \langle \downarrow, \downarrow, \dots, \downarrow | \mathbf{n} \rangle. \quad (\text{E2})$$

Furthermore, the straightforward calculations yield that

$$P_H^{(1)}(\mathbf{n}) = \prod_{j=1}^N \frac{\cos(\theta_j/2)^2}{2\pi}; \quad (\text{E3})$$

$$P_H^{(2)}(\mathbf{n}) = \prod_{j=1}^N \frac{\sin(\theta_j/2)^2}{2\pi}; \quad (\text{E4})$$

$$|P_H^{(3)}(\mathbf{n})| = \prod_{j=1}^N \frac{\sin(\theta_j/2) \cos(\theta_j/2)}{2\pi}, \quad (\text{E5})$$

where $\theta_j \in [0, \pi]$ is the polar angle of \mathbf{n}_j , with $\mathbf{n} \equiv (\mathbf{n}_1, \mathbf{n}_2, \dots, \mathbf{n}_N)$, as shown in Sec. II. Eqs (E3-E5) show that when $N \rightarrow \infty$, the functions $P_H^{(1)}(\mathbf{n})$ and $P_H^{(2)}(\mathbf{n})$ significantly at the points with $\theta_1 = \theta_2 = \dots = \theta_N = 0$ and $\theta_1 = \theta_2 = \dots = \theta_N = \pi$, respectively. So we suppose that the contributions of $P_H^{(1,2)}(\mathbf{n})$ to the integral of the expression (8) of the Wehrl entropy are mainly given by that of the regions around these two peaking points. Moreover, the maximum value of $|P_H^{(3)}(\mathbf{n})|$ ($(4\pi)^{-N}$) is much less the peaking values of $P_H^{(1,2)}(\mathbf{n})$ ($(2\pi)^{-N}$). Therefore, in the calculation of the Wehrl entropy with Eq. (8) we totally ignore the contributions from $P_H^{(3)}(\mathbf{n})$. The similar analysis yields that in this calculation one can also ignore $P_H^{(1)}(\mathbf{n})$ in the regions around the peaking point of $P_H^{(2)}(\mathbf{n})$, and vice versa. Thus, in the

limit $N \rightarrow \infty$ the Wehrl entropy of the GHZ states is

$$\begin{aligned} S_W(\hat{\rho}) &\approx -\frac{1}{2} \int P_H^{(1)}(\hat{\rho}; \mathbf{n}) \ln \left[P_H^{(1)}(\hat{\rho}; \mathbf{n})/2 \right] d\mathbf{n} \\ &\quad -\frac{1}{2} \int P_H^{(2)}(\hat{\rho}; \mathbf{n}) \ln \left[P_H^{(2)}(\hat{\rho}; \mathbf{n})/2 \right] d\mathbf{n} \\ &= \ln 2 + \Lambda_L N, \end{aligned} \quad (\text{E6})$$

which yields $\lim_{N \rightarrow \infty} S_W(\hat{\rho})/N = \Lambda_L$ and $S_W/N \approx (\ln 2)/N + \Lambda_L$ in the large- N limit.

Now we consider the R2 states defined in Sec. VC. The density operator $\hat{\rho} = |\text{R2}\rangle\langle\text{R2}|$ of this state can be expressed as a density matrix in the basis $\{|s_1, s_2, \dots, s_N\rangle, s_1, s_2, \dots, s_N = \uparrow, \downarrow\}$ the density operator $\hat{\rho} = |\text{R2}\rangle\langle\text{R2}|$. The diagonal elements of this density matrix are all $1/2^N$. The norm of the non-diagonal elements are also $1/2^N$, but the complex phases of the non-diagonal elements are very random when $N \rightarrow \infty$, due to the random phases $\phi_{s_1, s_2, \dots, s_N}$ in the expression (24) of this state. On the other hand, in the calculations of the Wehrl entropy with Eq. (8), there are summations for the these non-diagonal matrix elements. Due to these random phases we suppose that these summations can be ignored in the limit $N \rightarrow \infty$, and thus in the calculation of the Wehrl entropy one can only keep the diagonal elements of the density matrix, *i.e.*, make the approximation $S_W(\hat{\rho}) \approx S_W(\hat{\rho}')$, with $\hat{\rho}' = \sum_{s_1, s_2, \dots, s_N = \uparrow, \downarrow} |s_1, s_2, \dots, s_N\rangle\langle s_1, s_2, \dots, s_N| / (2\pi)^{N/2}$. It is clear that $\hat{\rho}'$ is just the density operator of the maximum mixed state, *i.e.*, $\hat{\rho} = \bigotimes_{j=1}^N (\hat{I}_j/2)$, where \hat{I}_j ($j = 1, \dots, N$) is the identity operator for particle j . Thus, we have $S_W(\hat{\rho})/N \approx \Lambda_U$.

Moreover, an analysis similar to above also implies that $S_W(\hat{\rho})/N \approx \Lambda_U$ for the R1 states.

-
- [1] A. Wehrl, *Reviews of Modern Physics* **50**, 221 (1978).
[2] M. A. Nielsen and I. L. Chuang, *Quantum Computation and Quantum Information* (Cambridge University Press, 2012).
[3] B. Zeng, X. Chen, D.-L. Zhou, and X.-G. Wen, *Quantum Information Meets Quantum Matter* (Springer New York, 2019).
[4] K. Huang, *STATISTICAL MECHANICS* (Wiley, 1987).
[5] X. Han and B. Wu, *Physical Review E* **91**, 062106 (2015).
[6] Z. Hu, Z. Wang, and B. Wu, *Physical Review E* **99**, 052117 (2019).
[7] A. Wehrl, *Reports on Mathematical Physics* **16**, 353 (1979).
[8] K. Husimi, *Proc. Phys. Math. Soc. Jpn.* **22**, 264 (1940).
[9] A. Orłowski, H. Paul, and G. Kastelewick, *Physical Review A* **52**, 1621 (1995).
[10] B. O. Goes, G. T. Landi, E. Solano, M. Sanz, and L. C. Céleri, *Physical Review Research* **2**, 033419 (2020).
[11] F. Mintert and K. Życzkowski, *Physical Review A* **69**, 022317 (2004).
[12] E. H. Lieb, *Communications in Mathematical Physics* **62**, 35 (1978).
[13] C. T. Lee, *Journal of Physics A: Mathematical and General* **21**, 3749 (1988).
[14] A. Sugita, *Journal of Physics A: Mathematical and General* **36**, 9081 (2003).
[15] E. H. Lieb and J. P. Solovej, *Acta Mathematica* **212**, 379 (2014).
[16] Explicitly, we use the fitting function $A + B/N + C/N^2$. Thus, the value of A given by the fitting is the Wehrl entropy per particle in the limit $N \rightarrow \infty$. The fitting results we obtained are $A = 2.53313 \pm 0.00444$ for the R1/R2/R3 states, $A = 2.33226 \pm 0.01798$ for the GHZ states, and 2.34337 ± 0.01782 for the W states.
[17] In the ‘‘classical version’’ of the thought experiment in Sec. III for $N = 1$, there are m copies $t^{(1)}, t^{(2)}, \dots, t^{(m)}$ of the charged spinning top, with each one having the same phase-space probability distribution $P_C(\mathbf{n})$. The experimenter choose m independent random directions $\mathbf{u}^{(1)}, \mathbf{u}^{(2)}, \dots, \mathbf{u}^{(m)}$ from S^2 , and measure the projection of the symmetry axis direction \mathbf{w} on the direction $\mathbf{u}^{(\eta)}$ (*i.e.*, the value of $\mathbf{w} \cdot \mathbf{u}^{(\eta)}$) for the copy $t^{(\eta)}$ ($\eta = 1, \dots, m$).

If the outcome is +1, then experimenter denote the direction $\hat{\mathbf{u}}^{(\eta)}$ in the notebook. Now the question is, after all the measurements, the number of the denoted direc-

tions in a small solid angle $\Delta\Omega$ around direction \mathbf{n} is $D\Delta\Omega\mathcal{P}(\mathbf{u} = \mathbf{n} | \mathbf{w} = \mathbf{u})$, with D being the total number of all the denoted directions.